CHAPTER

9

The Geometry Outside a Spherical Star

The simplest curved spacetimes of general relativity are the ones with the most symmetry, and the most useful of these is the geometry of empty space outside a spherically symmetric source of curvature, for example, a spherical star. This is called the *Schwarzschild geometry* after Karl Schwarzschild (1873–1916), who solved the Einstein equation to find it in 1916. To an excellent approximation this is the curved spacetime outside the Sun and therefore leads to the predictions of Einstein's theory most accessible to experimental test. We show in Chapter 21 that the Schwarzschild geometry is a solution of the vacuum Einstein equation—the Einstein equation for curved spacetime devoid of matter. In this chapter we explore the geometry of Schwarzschild's solution, assuming it's given. We will concentrate on the predicting the orbits of test particles and light rays in the curved spacetime of a spherical star that exhibit some of the famous effects of general relativity—the gravitational redshift, the precession of the perihelion of a planet, the gravitational bending of light, and the time delay of light. The next chapter describes experiments and observations that check these predictions and test Einstein's theory.

9.1 Schwarzschild Geometry

In a particularly suitable set of coordinates, the line element summarizing the Schwarzschild geometry is given by ($c \neq 1$ units)

Schwarzschild Metric

$$ds^2 = -\left(1 - \frac{2GM}{c^2 r}\right)(c\,dt)^2 + \left(1 - \frac{2GM}{c^2 r}\right)^{-1} dr^2 + r^2\left(d\theta^2 + \sin^2\theta\, d\phi^2\right). \tag{9.1}$$

The coordinates are called *Schwarzschild coordinates* and the corresponding metric $g_{\alpha\beta}(x)$ is called the *Schwarzschild metric*. It has the following important properties:

- *Time Independent* The metric is independent of t. There is a Killing vector $\boldsymbol{\xi}$ associated with this symmetry under displacements in the coordinate time t, which has the components [cf. (8.27)]

$$\xi^\alpha = (1, 0, 0, 0) \tag{9.2}$$

(listed in the order (t, r, θ, ϕ)) in the coordinate basis associated with (9.1).

- *Spherically Symmetric* The geometry of a two-dimensional surface of constant t and constant r in the four-dimensional geometry (9.1) is summarized by the line element

$$d\Sigma^2 = r^2(d\theta^2 + \sin^2\theta\, d\phi^2). \tag{9.3}$$

This describes the geometry of a sphere of radius r in flat three-dimensional space [cf. (2.15)]. The Schwarzschild geometry thus has the symmetries of a sphere with regard to changes in the angles θ and ϕ. In (9.1) or (9.3) this is evident for the ϕ-direction because the metric is independent of ϕ—invariant under rotations about the z-axis. The Killing vector associated with this symmetry is [cf. (8.27)]

$$\eta^\alpha = (0, 0, 0, 1). \tag{9.4}$$

There are Killing vectors associated with the other rotational symmetries but we won't need them.

The Schwarzschild coordinate r has a simple geometric interpretation arising from spherical symmetry. It is *not* the distance from any "center." Rather, it is related to the area A of the two-dimensional spheres of fixed r and t by the standard formula

$$r = (A/4\pi)^{1/2}. \tag{9.5}$$

This follows from (9.3), (7.28), and (7.37).

- *Mass M* If GM/c^2r is small, the coefficient of dr^2 in the line element (9.1) can be expanded to give

$$ds^2 \approx -\left(1 - \frac{2GM}{c^2r}\right)(c\,dt)^2 + \left(1 + \frac{2GM}{c^2r}\right)dr^2 + r^2\left(d\theta^2 + \sin^2\theta\, d\phi^2\right). \tag{9.6}$$

This is exactly the form of the static, weak field metric (6.20) with a Newtonian gravitational potential Φ given by

$$\Phi = -\frac{GM}{r}. \tag{9.7}$$

This leads to the identification of the constant M in the Schwarzschild metric (9.1) with the *total mass* of the source of curvature.

In Newtonian physics the Sun's mass is determined by measuring the period and size of the orbit of a test body (the Earth) and using Kepler's law [cf. (3.24)] to relate these to the mass of the source of gravitational attraction. In general relativity the mass of a stationary source of spacetime curvature is *defined* by this kind of experiment. Any form of energy is a source of spacetime curvature, including the energy in electromagnetic fields, nuclear interaction energy, etc., and, in a rough sense that will be clearer later, the energy in spacetime curvature itself. The limit of very large orbits should, therefore, be taken to define a *total mass*, that includes all of these. The larger the orbit, the more accurately its properties are determined by the Newtonian approximation as (9.6) and the discussion in Section 6.6 show. The total mass of a stationary body can, therefore, be defined by Kepler's law for a very large orbit, and, since that is determined by the Newtonian potential (9.7), the constant M in the Schwarzschild metric (9.1) is the total mass.

The geometry outside a spherically symmetric source is thus characterized by a single number—the total mass M—and not on how that mass is radially distributed inside the source. That's the relativistic version of Newton's theorem for the Newtonian gravitational potential discussed in Example 3.1.

- *Schwarzschild Radius* There is obviously something interesting happening to the metric at the radii $r = 0$ and $r = 2GM/c^2$. The latter is called the *Schwarzschild radius* and is the characteristic length scale for curvature in the Schwarzschild geometry. It turns out, however, that the surface of a static star is always outside these radii. The Schwarzschild radius of the Sun, for instance, is $2GM_{\odot}/c^2 = 2.95$ km—much smaller than the radius of the solar surface 6.96×10^5 km. At the surface the Schwarzschild geometry joins a different geometry inside the star. As long as one sticks to the outsides of static stars, one doesn't have to worry about the radii $r = 2GM/c^2$ and $r = 0$. However, we will have to face up these radii in Chapter 12 when we consider the gravitational collapse of a star to zero radius and the formation of a black hole.

Equation (9.1) exhibits the Schwarzschild geometry in mass-length-time ($\mathcal{MLT}$) units. The expression is a little simpler in the $\mathcal{ML}$ units that are convenient for special relativity, where $c = 1$ and both and space and time have the same dimension of length. A system of units convenient for general relativity also puts $G = 1$ by measuring mass in units of length through the conversion

$$M(\text{in cm}) = \frac{G}{c^2} M(\text{in g}) = .742 \times 10^{-28} \left(\frac{\text{cm}}{\text{g}}\right) M(\text{in g}). \tag{9.8}$$

Geometrized Units

In these units, for example, the mass of the Sun is $M_{\odot} = 1.47$ km and the mass of the Earth is $M_{\oplus} = .44$ cm. These $\mathcal{L}$ units are called *geometrized units*, or $c = G = 1$ units. To convert an expression in geometrized units back to $\mathcal{MLT}$ ones, it is necessary only to insert the correct factors of G and c, replacing, for example, M by GM/c^2, τ by $c\tau$, $dx^i/d\tau$ by $(1/c)(dx^i/d\tau)$, etc. Appendix A gives a list of such transformation rules as well as a brief general discussion of units.[1]

[1] Does this discussion mean that the value of Newton's constant can be defined like the value of c is? Not at present because the unit of gravitational mass is defined in terms of inertial mass—the standard kilogram—whose gravitational properties are determined by measurement. See the discussion in Appendix A.

In geometrized units the Schwarzschild line element has the form

$$\boxed{ds^2 = -\left(1 - \frac{2M}{r}\right) dt^2 + \left(1 - \frac{2M}{r}\right)^{-1} dr^2 + r^2 \left(d\theta^2 + \sin^2\theta \, d\phi^2\right).} \tag{9.9}$$

Schwarzschild Metric (geometrical units)

Explicitly the metric $g_{\alpha\beta}$ is

$$g_{\alpha\beta} = \begin{array}{c} \\ t \\ r \\ \theta \\ \phi \end{array} \begin{array}{c} \begin{array}{cccc} \quad t \quad & \quad r \quad & \theta & \phi \end{array} \\ \begin{pmatrix} -(1-2M/r) & 0 & 0 & 0 \\ 0 & (1-2M/r)^{-1} & 0 & 0 \\ 0 & 0 & r^2 & 0 \\ 0 & 0 & 0 & r^2\sin^2\theta \end{pmatrix} \end{array} . \tag{9.10}$$

Both theoretically and experimentally the Schwarzschild geometry can be studied through the orbits of test particles and light rays. Observations of the small effects predicted by general relativity on the orbits of planets and trajectories of light rays in the solar system are important tests of the theory. The following discussion concentrates on the effects that lead to experimental tests beginning with the gravitational redshift.

9.2 The Gravitational Redshift

Consider an observer stationed at a fixed Schwarzschild coordinate radius R who emits a light signal. When emitted, the signal has frequency ω_* as measured by this stationary observer. The light signal propagates out to infinity, not necessarily along a radial path, where its frequency is measured by another stationary observer (see Figure 9.1). The frequency ω_∞ received by an observer at infinity is less than ω_*. That is the gravitational redshift worked out from the equivalence principle to first order in $1/c^2$ in Example 6.2. The following discussion derives it exactly in the Schwarzschild geometry.

The change in frequency is related to the change in energy of an emitted photon because for any observer, $E = \hbar\omega$. In Newtonian physics the change in kinetic energy of a particle moving in a time-independent potential can be easily calculated from the conservation of energy arising from time-displacement invariance. This suggests that the efficient way to calculate the change in frequency of a photon moving in the time-independent Schwarzschild geometry is to make use of the conserved quantity that arises because of its time-displacement invariance. This conserved quantity is $\boldsymbol{\xi} \cdot \mathbf{p}$ [cf. (8.32)], where $\mathbf{p}$ is the photon's four-momentum and $\boldsymbol{\xi}$ is the Killing vector (9.2) associated with time-displacement symmetry. Let's see how to do that.

The energy of the photon measured by an observer with four-velocity $\mathbf{u}_{\text{obs}}$ is

$$E = -\mathbf{p} \cdot \mathbf{u}_{\text{obs}}, \tag{9.11}$$

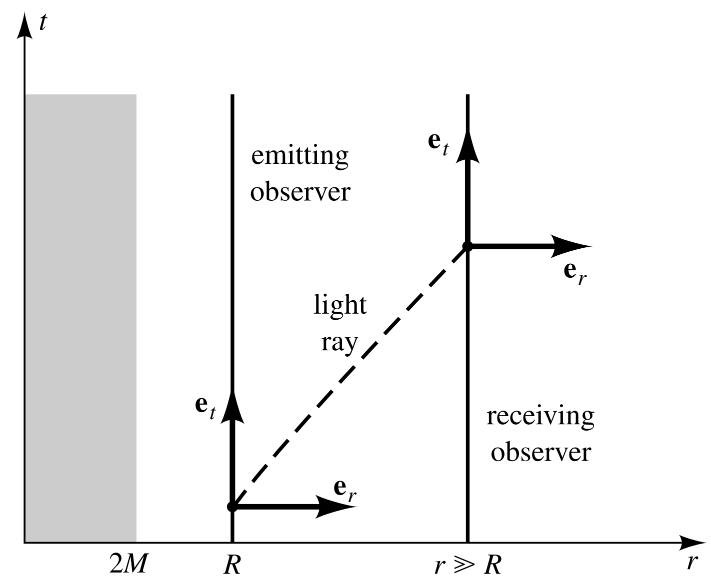

FIGURE 9.1 A spacetime diagram showing the world lines of two stationary observers outside of a spherically symmetric mass. One observer hovers at radius R, the other is "at infinity," that is, at a radius $r \gg R$. A photon is emitted from radius R with frequency ω_* as measured in the laboratory of a stationary observer at R. The photon propagates along the dotted world line until it is detected by the observer at infinity with frequency ω. Two of the orthonormal vectors associated with each laboratory are indicated schematically. The frequency ω_∞ is less than ω_* because the photon loses energy climbing out of the gravitational well of the central mass. That is the gravitational redshift.

as described in (7.53) and the discussion following it. Since the energy of a photon is related to its frequency by $E = \hbar\omega$,

$$\hbar\omega = -\mathbf{p} \cdot \mathbf{u}_{\text{obs}}, \tag{9.12}$$

giving the frequency measured by an observer with four-velocity $\mathbf{u}_{\text{obs}}$. The spatial components u^i_{obs} of the four-velocity are zero for a stationary observer. The time component $u^t_{\text{obs}}(r)$ of a stationary observer at radius r is determined by the normalization condition [cf. (8.25)]

$$\mathbf{u}_{\text{obs}}(r) \cdot \mathbf{u}_{\text{obs}}(r) = g_{\alpha\beta} u^\alpha_{\text{obs}}(r) u^\beta_{\text{obs}}(r) = -1. \tag{9.13}$$

Since $u^i_{\text{obs}}(r) = 0$, this implies

$$g_{tt}(r)[u^t_{\text{obs}}(r)]^2 = -1, \tag{9.14}$$

and, using the metric (9.10), this gives

$$u^t_{\text{obs}}(r) = \left(1 - \frac{2M}{r}\right)^{-1/2}. \tag{9.15}$$

Thus,

$$u^\alpha_{\text{obs}}(r) = [(1 - 2M/r)^{-1/2}, 0, 0, 0] = (1 - 2M/r)^{-1/2}\xi^\alpha, \tag{9.16}$$

where $\boldsymbol{\xi}$ is the Killing vector (9.2) associated with the time independence of the Schwarzschild metric. For a stationary observer at radius r, therefore,

$$\mathbf{u}_{\text{obs}}(r) = (1 - 2M/r)^{-1/2}\boldsymbol{\xi}. \tag{9.17}$$

Using (9.17) in (9.12), the frequency of the photon measured by the stationary observer at radius R is,

$$\hbar\omega_* = \left(1 - \frac{2M}{R}\right)^{-1/2} (-\boldsymbol{\xi} \cdot \mathbf{p})_R, \tag{9.18}$$

where the subscript R indicates that the quantities are to be evaluated at a Schwarzschild radius R. Similarly, at infinite radius

$$\hbar\omega_\infty = (-\boldsymbol{\xi} \cdot \mathbf{p})_\infty. \tag{9.19}$$

But from (8.32) the quantity $\boldsymbol{\xi} \cdot \mathbf{p}$ is *conserved* along the photon's geodesic. It is the same at infinity as it is at radius R. The frequencies are, therefore, related by

$$\boxed{\omega_\infty = \omega_* \left(1 - \frac{2M}{R}\right)^{1/2}.} \tag{9.20}$$

Gravitational Redshift

The frequency at infinity is *less* than the frequency at R by a factor $(1-2M/R)^{1/2}$. The photon has suffered a gravitational redshift.

Equation (9.20) may be expanded in powers of $2M/R$ when that is small, as for the Sun. The first two terms reproduce the approximate result (6.14) derived from the principle of equivalence.

9.3 Particle Orbits—Precession of the Perihelion

Let's now examine the orbits of test particles following timelike geodesics in the Schwarzschild geometry. These test particles might be the planets orbiting our Sun or particles of an the accretion disk orbiting a neutron star or black hole.

Conserved Quantities

The study of geodesics in the Schwarzschild geometry is considerably aided by the laws of conservation of energy and angular momentum that hold because the metric is independent of time and spherically symmetric. In particular, since the metric is independent of t and ϕ, the quantities $\boldsymbol{\xi} \cdot \mathbf{u}$ and $\boldsymbol{\eta} \cdot \mathbf{u}$ are conserved [cf. (8.32)], where $\mathbf{u}$ is the four-velocity of the particle and $\boldsymbol{\xi}$ and $\boldsymbol{\eta}$ are given by (9.2) and (9.4). These quantities are so useful it is convenient to give them special

BOX 9.1 Time Machines

In science fiction, time machines transport a traveler forward or backward in time. General relativity—the theory of space and time—supplies the principles for analyzing whether time machines are possible and practical.

Relativity provides several examples of time machines that transport an observer to events in the future faster than other observers. The twin paradox setup discussed on p. 63 is the simplest example. As viewed in an inertial frame in flat spacetime, one twin accelerates away from a stationary twin, reaches speeds close to the velocity of light, and returns. The accelerating twin returns younger than the stationary twin who follows a geodesic—the curve of *longest* proper time. If accelerated to high enough velocities, the returning twin can participate in events far to the future of the lifetime of any stationary human observer. That is transportation forward in time. *Any* spacetime therefore abounds in forward time machines—two points that can be connected by timelike curves with two different lengths.

Curved spacetime provides different kinds of forward time machines. Construct a spherical shell of mass M and radius R and go live inside. The exterior geometry is Schwarzschild. Inside spacetime is flat. (There would be no force in Newtonian gravity because there is no mass inside any sphere of symmetry. This also holds in relativity.) Your clocks inside the shell will run slower than clocks at infinity by the gravitational redshift factor $(1 - 2M/R)^{1/2}$ [cf. (9.20)]. Suppose, for example, you wanted to know by the end of a day the output of a computation that would take a hundred years to carry out on your laptop. Or suppose that you wanted to watch the next hundred years of television in a day. Leave your laptop and television outside the shell and go inside the shell to watch. How big and how massive a shell would you need to construct? You would need an M and R such that $(1-2M/R)^{1/2} = 1/(100 \times 365) \approx 3 \times 10^{-5}$. That is, the radius of the shell R could only be very *slightly* bigger than twice its mass M. Assuming that one needs a reasonable-size living room inside of, say, $R \sim 10$ m, the mass required would be $M \approx 5$ m $\approx (1/300)M_\odot$ or a shell 4 times the mass of Jupiter. There is no material that would support the resulting stress, and the shell has to be considerably larger and much more massive to have low enough stresses (Problem 4).

In Chapter 12 we will learn that a shell is not really needed to construct a forward time machine. Hovering outside a black hole near $R = 2M$ is equally effective. That, however, requires an expenditure of energy to create the thrust to balance the gravitational attraction of a black hole. The no-cost option is to fall freely into the black hole. But then one can never return, and the maximum time to view the future even for the largest black holes in the known universe is about three hours before destruction in a singularity.

What about traveling backward in time? The world line of an observer can't turn backwards in time because to do so, it would have to be moving faster than the speed of light at some point. The only way to travel backward in time to an earlier point in one's history is if spacetime has closed timelike curves. It's possible to cook up spacetimes with this property. Take flat spacetime in a particular Lorentz frame and identify points along the $t = 0$ surface with points on a $t = T$ surface. Spacetime is then curled up in the t-direction like a cylinder, and closed timelike curves of constant $\vec{x}$ go around it. But there is no evidence that our universe has such an exotic topological structure, and, if energy is positive, general relativity prohibits the evolution of closed timelike curves in a space with a simple topological structure like the one we believe we live in. Thus, although it is possible in principle to go forward into the future, we probably cannot revisit the past, at least in the classical theory of gravity.

names. We'll call them[2] $-e$ and ℓ. Their explicit forms are

$$\boxed{e = -\boldsymbol{\xi} \cdot \mathbf{u} = \left(1 - \frac{2M}{r}\right) \frac{dt}{d\tau},} \tag{9.21}$$

Conserved Energy per Unit Rest Mass

$$\boxed{\ell = \boldsymbol{\eta} \cdot \mathbf{u} = r^2 \sin^2\theta \frac{d\phi}{d\tau}.} \tag{9.22}$$

Conserved Angular Momentum per Unit Rest Mass

At large r the constant e becomes energy per unit rest mass because in flat space, $E = mu^t = m(dt/d\tau)$ [cf. (5.41)]. Energy per unit rest mass is what we'll call it everywhere. We'll call the conserved quantity ℓ the angular momentum per unit rest mass because that's what it is at low velocities. Thus, there is a conserved energy and angular momentum for particle orbits.

Effective Potential and Radial Equation

The conservation of angular momentum implies that the orbits lie in a "plane," as do the orbits in Newtonian theory. To see this, fix your attention on a particular instant and let $\vec{u}$ denote the spatial components of the particle's four-velocity. Orient the coordinates so $d\phi/d\tau = 0$ at that instant and the particle is at $\phi = 0$, i.e., so that $\vec{u}$ lies in the meridional "plane" $\phi = 0$. According to (9.22) this implies $\ell = 0$, so that $d\phi/d\tau$ is zero everywhere along the geodesic. The particle thus remains in the meridional "plane" $\phi = 0$. Having once established this, it is simpler to reorient the coordinates so that the particle orbits are in the equatorial "plane." Thus for the rest of the discussion we consider $\theta = \pi/2$ and $u^\theta = 0$.

Orbits in a Plane

The normalization of the four-velocity supplies another integral for the geodesic equation in addition to those for energy (9.21) and angular momentum (9.22). Explicitly, this third integral reads

$$\mathbf{u} \cdot \mathbf{u} = g_{\alpha\beta} u^\alpha u^\beta = -1. \tag{9.23}$$

These three integrals can be used to express the three nonzero components of the four-velocity in terms of the constants of the motion e and ℓ. Writing (9.23) out for the Schwarzschild metric (9.10), and taking account of the equatorial plane condition $u^\theta = 0$, $\theta = \pi/2$ gives

$$-\left(1 - \frac{2M}{r}\right)(u^t)^2 + \left(1 - \frac{2M}{r}\right)^{-1}(u^r)^2 + r^2 (u^\phi)^2 = -1. \tag{9.24}$$

Writing $u^t = dt/d\tau$, $u^r = dr/d\tau$, and $u^\phi = d\phi/d\tau$ and using (9.21) and (9.22) to eliminate $dt/d\tau$ and $d\phi/d\tau$, (9.24) can be rewritten as

[2] Don't get e mixed up with the eccentricity of an orbit. We'll denote that by ϵ.

$$-\left(1-\frac{2M}{r}\right)^{-1}e^2+\left(1-\frac{2M}{r}\right)^{-1}\left(\frac{dr}{d\tau}\right)^2+\frac{\ell^2}{r^2}=-1. \tag{9.25}$$

With a little further rewriting, this can be put in the form

$$\frac{e^2-1}{2}=\frac{1}{2}\left(\frac{dr}{d\tau}\right)^2+\frac{1}{2}\left[\left(1-\frac{2M}{r}\right)\left(1+\frac{\ell^2}{r^2}\right)-1\right]. \tag{9.26}$$

We have written the expression in this form to show the correspondence with the energy integral of Newtonian mechanics. By defining the constant

$$\mathcal{E}\equiv(e^2-1)/2 \tag{9.27}$$

and the effective potential

Effective Potential for Radial Motion of Particles

$$\boxed{V_{\text{eff}}(r)\equiv\frac{1}{2}\left[\left(1-\frac{2M}{r}\right)\left(1+\frac{\ell^2}{r^2}\right)-1\right]=-\frac{M}{r}+\frac{\ell^2}{2r^2}-\frac{M\ell^2}{r^3}} \tag{9.28}$$

the correspondence becomes exact:

$$\boxed{\mathcal{E}=\frac{1}{2}\left(\frac{dr}{d\tau}\right)^2+V_{\text{eff}}(r).} \tag{9.29}$$

Thus, the techniques for treating orbits by effective potentials in Newtonian mechanics can be applied to the orbits in the Schwarzschild geometry. Indeed the form of the effective potential (9.28) differs from that of a $-M/r$ Newtonian central potential by only the additional $-M\ell^2/r^3$ term. That term, however, will have important consequences for orbits, as we explore shortly.

Greater insights into (9.29) may be obtained by considering its nonrelativistic limit. To do this, first put back the factors of c and G by replacing t and τ by ct and $c\tau$ and by replacing M by GM/c^2. The conserved quantity ℓ is replaced by ℓ/c, where ℓ continues to mean $r^2(d\phi/d\tau)$. The effective potential $V_{\text{eff}}(r)$ becomes

$$V_{\text{eff}}(r)=\frac{1}{c^2}\left(-\frac{GM}{r}+\frac{\ell^2}{2r^2}-\frac{GM\ell^2}{c^2r^3}\right). \tag{9.30}$$

The dimensionless constant e is the total energy per unit rest mass. Anticipating a correspondence with the usual Newtonian energy, let's define E_{Newt} by

$$e\equiv\frac{mc^2+E_{\text{Newt}}}{mc^2}. \tag{9.31}$$

Using (9.30) and (9.31), (9.29) becomes

$$E_{\text{Newt}} = \frac{m}{2}\left(\frac{dr}{d\tau}\right)^2 + \frac{L^2}{2mr^2} - \frac{GMm}{r} - \frac{GML^2}{c^2mr^3}, \tag{9.32}$$

where $L = m\ell$. This has the same form as the energy integral in Newtonian gravity with an additional relativistic correction to the potential proportional to $1/r^3$. The Newtonian limit is recovered when this relativistic derivative is dropped and τ-derivatives can be replaced by t-derivatives.

Returning to the analysis of the relativistic orbits, consider the properties of the effective potential $V_{\text{eff}}(r)$. A few simple properties are immediate from its definition (9.28):

$$V_{\text{eff}}(r) \underset{r\to\infty}{\rightarrow} -\frac{M}{r}, \qquad V_{\text{eff}}(2M) = -\frac{1}{2}. \tag{9.33}$$

For large values of r the potential is close to the Newtonian effective potential for motion in a $1/r$ potential, as Figure 9.2 illustrates. That is because the first two terms in (9.28) are the same as in Newtonian theory. However, as r decreases, the attractive $1/r^3$ correction from general relativity becomes increasingly important.

The extrema of the effective potential can be found from solving $dV_{\text{eff}}/dr = 0$. There is one local minimum and one local maximum, whose radii r_{min} and r_{max} are

$$r_{\substack{\text{min}\\ \text{max}}} = \frac{\ell^2}{2M}\left[1 \pm \sqrt{1 - 12\left(\frac{M}{\ell}\right)^2}\,\right]. \tag{9.34}$$

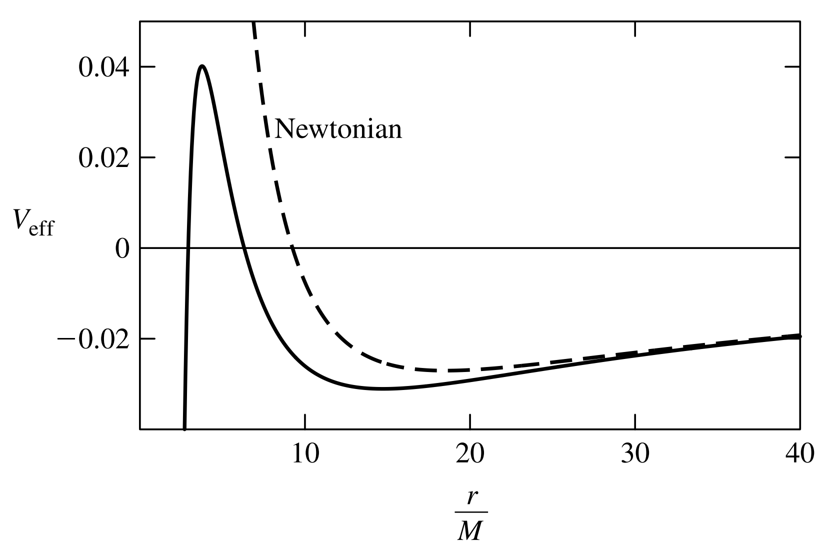

FIGURE 9.2 The relativistic and Newtonian effective potentials for radial motion compared for $\ell/M = 4.3$. The relativistic effective potential $V_{\text{eff}}(r)$ is defined by (9.28) and we take the Newtonian effective potential to be the first two terms of that. The two are close for large r, as shown, but differ significantly for small r, where the $1/r^3$ term in (9.28) becomes important. In particular the infinite centrifugal barrier of Newtonian theory becomes a barrier of finite height. For the Earth in orbit around the Sun, $\ell/M \sim 10^9$ and the differences between the Newtonian and relativistic potential over the orbit of the Earth are tiny but detectable in precise measurements, as we see in Chapter 10.

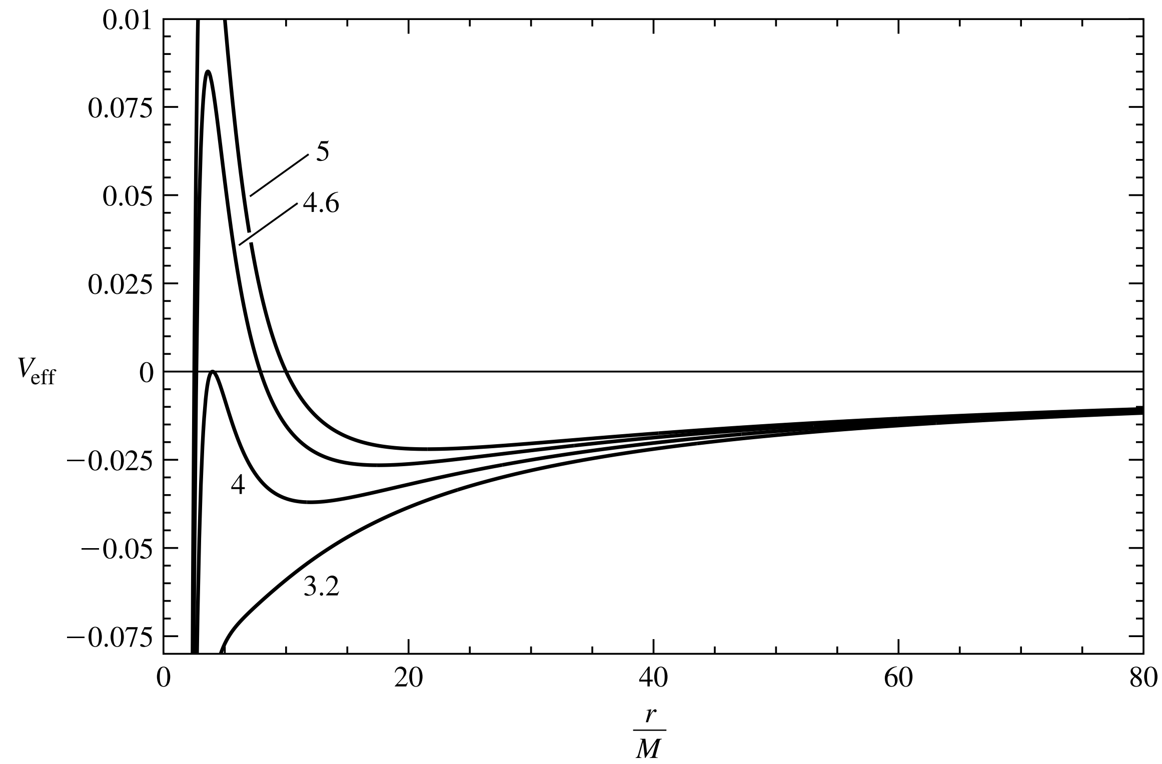

FIGURE 9.3 The effective potential $V_{\text{eff}}(r)$ for radial motion for several different values of ℓ. The values of ℓ/M label the curves.

Figure 9.3 is a plot of V_{eff} for various values of ℓ. If $\ell/M < \sqrt{12} = 3.46$, there are no real extrema and the effective potential is negative for all values of r. If $\ell/M > \sqrt{12}$ the effective potential has one maximum and one minimum. The maximum lies above $V_{\text{eff}} = 0$ if $\ell/M > 4$ and otherwise lies below it. There is a centrifugal barrier, but it has a maximum height, in contrast to the one in Newtonian theory that has infinite height. (See Figure 9.2.)

The qualitative behavior of an orbit depends on the relationship between $\mathcal{E} \equiv (e^2 - 1)/2$ and the effective potential in (9.29), just as in a Newtonian central force problem. Turning points occur at the radii r_{tp}, where $\mathcal{E} = V_{\text{eff}}(r_{\text{tp}})$, because that's where the radial velocity vanishes. If $\ell/M < \sqrt{12}$, there are no turning points for positive values of $\mathcal{E}$. An inwardly directed particle falls all the way to the origin. This is in contrast to Newtonian theory, where as long as $\ell \neq 0$ there is a positive centrifugal barrier that will reflect the particle (see Figure 9.2). Figure 9.4 shows four types of orbits for values of $\ell/M > \sqrt{12}$, along with their qualitative shapes. Circular orbits are possible at the radii (9.34) at which the effective potential has a maximum or a minimum. The orbit at the maximum is unstable because a small increase in $\mathcal{E}$ will lead the particle to escape to infinity or collapse to $r = 0$. The orbit at the minimum is stable. There are bound orbits for $\mathcal{E} < 0$ that oscillate between two turning points. (The planets are moving in bound orbits in the spacetime geometry of the Sun to a good approximation.) Orbits with positive $\mathcal{E}$ but less than the maximum of the effective potential are scattering orbits that come in from infinity, orbit the center of attraction, and then return.

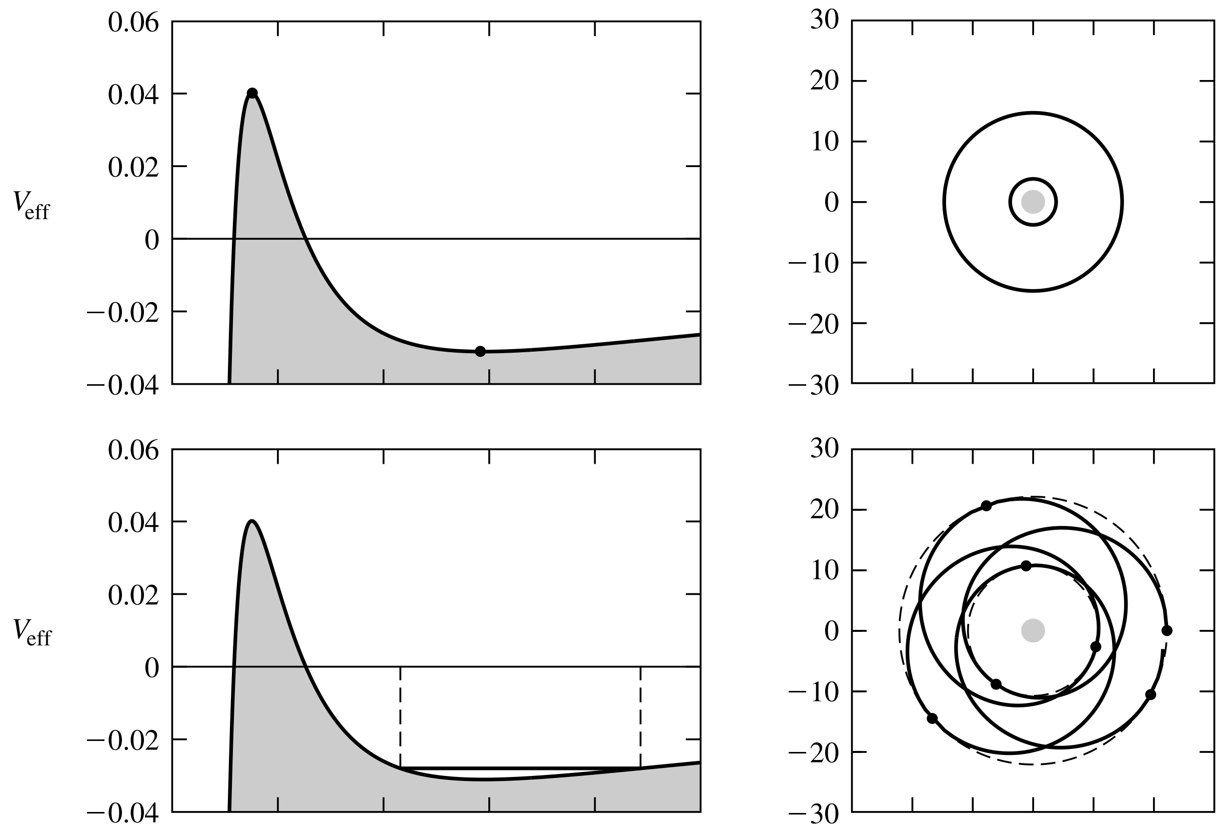

FIGURE 9.4 Four kinds of orbits in the Schwarzschild geometry. The pairs of figures on this page and the next show four orbits corresponding to different values of $\mathcal{E}$ for the illustrative value $\ell/M = 4.3$. The potential and its relationship to $\mathcal{E}$ are shown at left. The horizontal axis in these plots is r/M. The vertical axis is $V_{\text{eff}}(r)$. Horizontal lines indicate the values of $\mathcal{E}$. The vertical dashed lines are at turning points. The dots denote the possible locations of circular orbits. The shapes of the corresponding orbits are shown in the figures at right where Schwarzschild r and ϕ are plotted as polar coordinates in the plane. The shaded region at the center of each plot corresponds to $r < 2M$. The top figure on this page shows two circular orbits—the outer one is stable the inner one is unstable. The next figure shows a bound orbit in which the particle moves between two turning points marked by the dotted circles. The positions of closest approach (perihelion) and furthest excursion (aphelion) are indicated by dots. The precession of the perihelion is large for this relativistic orbit. (*Continued on next page.*)

Those with $\mathcal{E}$ greater than the maximum plunge into the center of attraction. In the following we will calculate the detailed properties of the orbits that are most important for future applications.

Radial Plunge Orbits

The simplest example of an orbit is the radial free fall of a particle from infinity—$\ell = 0$. The particle can start at infinity with various values of its kinetic energy corresponding to different positive values of $\mathcal{E}$, but starting from rest is an especially simple case. Then $dt/d\tau = 1$ at infinity, $e = 1$ from (9.21), or, equivalently, $\mathcal{E} = 0$ from (9.29).

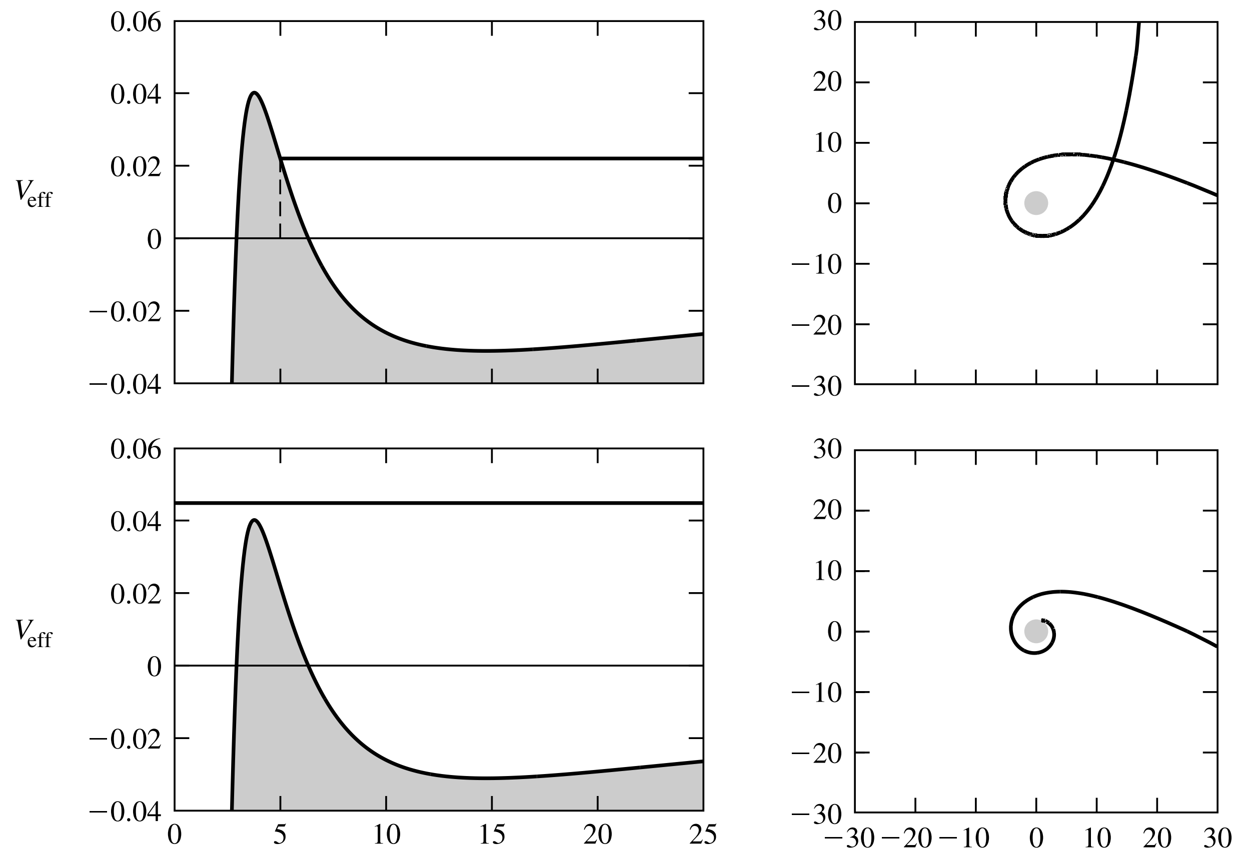

FIGURE 9.4 *continued.* The first figure on this page shows a scattering orbit. The particle comes in from infinity, passes around the center of attraction and moves out to infinity again. This is a highly relativistic orbit which differs significantly from a Newtonian parabola. The last pair of figures shows a plunge orbit in which the particle comes in from infinity moves part way around the central mass and then plunges into the center. This kind of orbit is not possible in Newtonian mechanics for a particle moving in a $1/r$ central potential.

From (9.26) with $e = 1$ and $\ell = 0$, we have

$$0 = \frac{1}{2}\left(\frac{dr}{d\tau}\right)^2 - \frac{M}{r}, \tag{9.35}$$

which gives the radial component of the four-velocity $dr/d\tau$. Taken together with the time component $dt/d\tau$ given by (9.21), the four-velocity is

$$u^\alpha = ((1 - 2M/r)^{-1}, -(2M/r)^{1/2}, 0, 0). \tag{9.36}$$

By writing (9.35) in the form

$$r^{1/2}dr = -(2M)^{1/2}d\tau, \tag{9.37}$$

both sides can be integrated to give r as a function of τ. The negative square root is appropriate for a geodesic going inward. The result is

$$r(\tau) = (3/2)^{2/3}(2M)^{1/3}(\tau_* - \tau)^{2/3}, \tag{9.38}$$

where τ_* is an arbitrary integration constant that fixes the proper time when $r = 0$. The Schwarzschild time can be conveniently found by first calculating t as a function of r and then using (9.38) to get it as a function of τ. Computing the derivative dt/dr from (9.21) with $e = 1$ and (9.35), we find

$$\frac{dt}{dr} = -\left(\frac{2M}{r}\right)^{-1/2}\left(1 - \frac{2M}{r}\right)^{-1}, \tag{9.39}$$

which on integration gives

$$t = t_* + 2M\left[-\frac{2}{3}\left(\frac{r}{2M}\right)^{3/2} - 2\left(\frac{r}{2M}\right)^{1/2} + \log\left|\frac{(r/2M)^{1/2}+1}{(r/2M)^{1/2}-1}\right|\right], \tag{9.40}$$

where t_* is another integration constant. There is thus a whole family of freely falling observers that start from rest at infinity. They may be labeled by giving the time they cross a particular radius or by giving their radius at a particular time. Either way this fixes t_*. The relation $t = t(\tau)$ can then be found by substituting (9.38) into (9.40).

Several important features of radial plunge orbits can be seen from (9.38) and (9.40). From (9.40), $r \to \infty$ as $t \to -\infty$, so the particle is falling inward from infinity. From (9.38) we see that from any fixed value of r on the trajectory, it takes only a finite proper time to reach $r = 2M$, even though (9.40) shows it takes an infinite amount of coordinate time t. This is just one indication that the Schwarzschild coordinates are flawed near $r = 2M$. Points are labeled by infinite coordinate values when they are actually only a finite distance away. We learn more about this in Chapter 12.

Example 9.1. Escape Velocity. An observer maintaining a stationary position at Schwarzschild coordinate radius R launches a projectile radially outward with velocity V, as measured in his or her own frame. How large does V have to be for the projectile to reach infinity with zero velocity? This is the escape velocity V_{escape}.

The outward-bound projectile follows a radial geodesic since there are no forces acting on it. At infinity a projectile at rest has $e = 1$. Since e is conserved, the observer must launch the projectile with a minimum value $e = 1$. This requires a four-velocity $\mathbf{u}$, which is the same as (9.35) but with the sign of u^r reversed. The energy E measured by the observer is $-\mathbf{p}\cdot\mathbf{u}_{\text{obs}}$ from (5.87), where $\mathbf{u}_{\text{obs}}$ is the stationary observer's four-velocity and $\mathbf{p} = m\mathbf{u}$ is the projectile's four momentum if m is its rest mass. The four-velocity of a stationary observer at radius R is given by (9.16). The result for the energy required at launch to escape is, therefore,

$$\begin{aligned} E &= -\mathbf{p}\cdot\mathbf{u}_{\text{obs}} = -m\mathbf{u}\cdot\mathbf{u}_{\text{obs}} = -mg_{\alpha\beta}u^\alpha u^\beta_{\text{obs}} \\ &= -mg_{tt}u^t u^t_{\text{obs}} = m\left(1 - \frac{2M}{R}\right)^{-1/2}. \end{aligned} \tag{9.41}$$

The fourth equality is because the four-velocity $\mathbf{u}_{\mathrm{obs}}$ of a stationary observer has only a t component and because the Schwarzschild metric is diagonal. The fifth is from substituting the values of the metric (9.10) and the four-velocities from (9.36) and (9.16). In the observer's frame the energy of a particle E is related to its speed V by $E = m/\sqrt{1-V^2}$ [cf. (5.46)]. Thus, the escape velocity is

$$V_{\mathrm{escape}} = \left(\frac{2M}{R}\right)^{1/2}. \tag{9.42}$$

This is, coincidently, the same formula as in Newtonian theory. As R approaches $2M$, the velocity necessary to escape approaches the velocity of light.

Stable Circular Orbits

Stable circular orbits occur at the radii $r = r_{\mathrm{min}}$ of the minima of the effective potential given in (9.34). These radii decrease with decreasing ℓ/M, but stable circular orbits are not possible at arbitrarily small radii. From (9.34), the innermost stable circular orbit (called the ISCO in relativistic astrophysics) in the Schwarzschild geometry occurs when $\ell/M = \sqrt{12}$ at the radius

Innermost Stable Circular Orbit

$$\boxed{r_{\mathrm{ISCO}} = 6M.} \tag{9.43}$$

That fact is important for the structure of X-ray sources, as we will see in Chapter 11.

The angular velocity of a particle in a circular orbit is the rate at which angular position in the orbit changes with time. The rate Ω with respect to the Schwarzschild coordinate time t is the rate measured with respect to a stationary clock at infinity, where t and the proper time of such a clock coincide. It is, for any equatorial orbit,

$$\Omega \equiv \frac{d\phi}{dt} = \frac{d\phi/d\tau}{dt/d\tau} = \frac{1}{r^2}\left(1-\frac{2M}{r}\right)\left(\frac{\ell}{e}\right), \tag{9.44}$$

where the last equality follows from (9.21) and (9.22). Circular orbits of radius r have values of ℓ and e determined by two requirements: First, the potential is a minimum at the radius of the orbit leading to the relation between r and ℓ in (9.34). Second, the value of $\mathcal{E}$ equals the value of the effective potential at that minimum. From (9.29) or (9.26) this gives $e^2 = (1-2M/r)(1+\ell^2/r^2)$. These two requirements can be solved for the ratio ℓ/e of circular orbits:

$$\frac{\ell}{e} = (Mr)^{1/2}\left(1-\frac{2M}{r}\right)^{-1} \qquad \text{(circular orbits)}. \tag{9.45}$$

Substituting this in (9.44) gives

Angular Velocity in Stable Circular Orbit

$$\boxed{\Omega^2 = \frac{M}{r^3} \qquad \text{(circular orbits).}} \tag{9.46}$$

This has the same form as the nonrelativistic Kepler's law. The period in Schwarzschild coordinate time is $2\pi/\Omega$, and (9.46) says that the square of the period is proportional to the cube of the radius of the orbit. This simple agreement between relativistic and nonrelativistic theory is, however, just a fortuitous consequence of the choice of Schwarzschild coordinate time to measure the angular velocity and Schwarzschild coordinate radius to measure the location of the orbit. The rate of change of angular position with respect to proper time, for example, is given by a more complicated formula (Problem 9).

The components of the four-velocity of a particle in a circular orbit are then

$$u^\alpha = u^t(1, 0, 0, \Omega) \tag{9.47}$$

with the angular velocity Ω given by (9.46). The component u^t is determined by the normalization condition $\mathbf{u} \cdot \mathbf{u} = -1$ in a way similar to (9.15) for a stationary observer. Now, however, there is a contribution from the angular velocity, and a similar calculation gives

$$u^t = \left(1 - \frac{2M}{r} - r^2\Omega^2\right)^{-1/2} = \left(1 - \frac{3M}{r}\right)^{-1/2} \quad \text{(circular orbits).} \tag{9.48}$$

The Shape of Bound Orbits

To find the shape of an orbit means finding r as a function of ϕ or, equivalently, ϕ as a function of r. To do this solve (9.29) for $dr/d\tau$, solve (9.22) with $\theta = \pi/2$ for $d\phi/d\tau$, and divide the first into the second. One finds

$$\frac{d\phi}{dr} = \pm\frac{\ell}{r^2}\frac{1}{[2(\mathcal{E} - V_{\text{eff}}(r))]^{1/2}} = \pm\frac{\ell}{r^2}\left[e^2 - \left(1 - \frac{2M}{r}\right)\left(1 + \frac{\ell^2}{r^2}\right)\right]^{-1/2}. \tag{9.49}$$

The sign corresponds to the direction in ϕ the particle moves with increasing r. The function $\phi(r)$ can be found simply by integrating the right-hand side. The result can be expressed in terms of elliptic functions but not in a very enlightening way for those not familiar with them. One especially important property is the question whether the orbits close. When we mention one *orbit* we will mean a passage between two successive inner turning points (or equivalently between two successive outer turning points). The orbits are said to *close* if the magnitude of the angle swept out in this passage $\Delta\phi$ is 2π. If it is not 2π, then the inner turning point is said to *precess*, and the amount of precession per orbit is

$$\delta\phi_{\text{prec}} = \Delta\phi - 2\pi. \tag{9.50}$$

as illustrated in Figure 9.6.

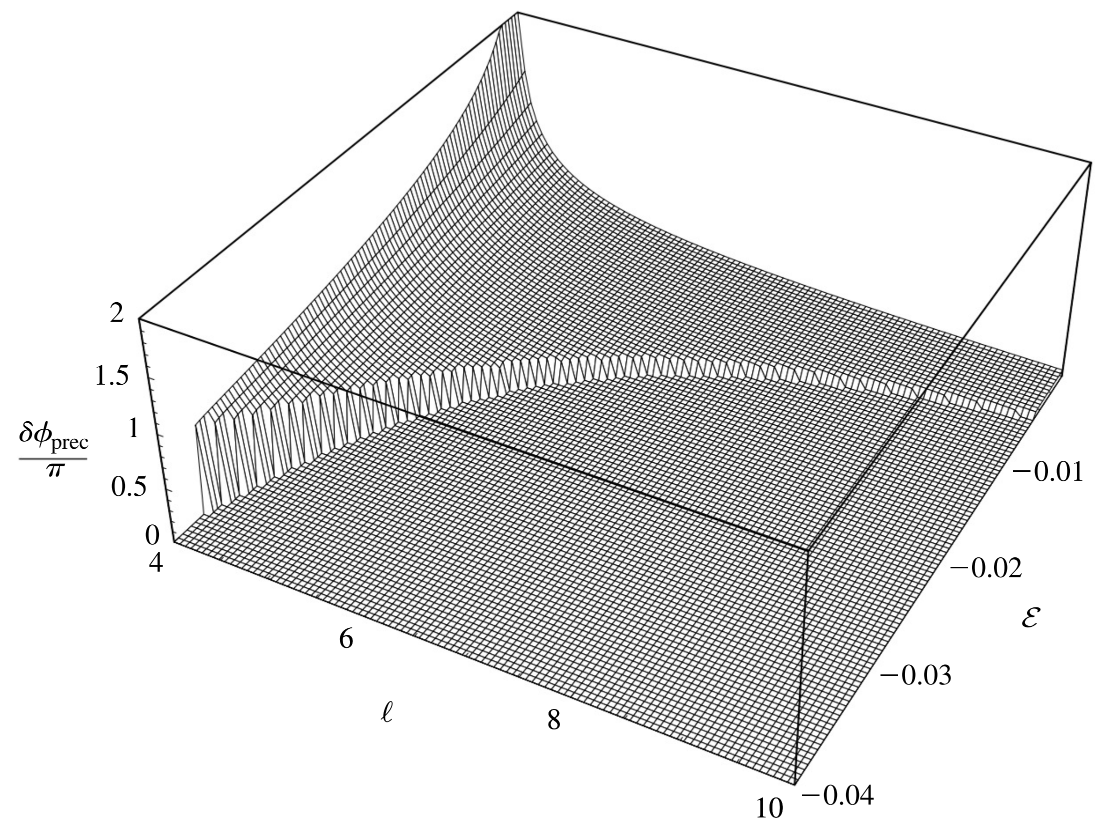

FIGURE 9.5 The precession of the perihelion $\delta\phi_{\text{prec}}$ in the Schwarzschild geometry for bound orbits characterized by the parameters $\mathcal{E} = (e^2 - 1)/2$ and ℓ. This is a plot of $\delta\phi_{\text{prec}}$ as defined by (9.50) and the integral (9.51). There are no bound orbits for the flat region in the foreground where $\delta\phi_{\text{prec}}$ is plotted as zero. The boundary is the curve of ℓ vs. e for circular orbits. Large values of ℓ correspond to orbits that are far from the star where relativistic effects are small. [See (9.45), for example, for the connection between ℓ and the radius of circular orbits.] That is the limit in which (9.57) is a good approximation, and the case important for the planets in the solar system.

The angle $\Delta\phi$ swept out in passing between successive inner turning points at r_1 is just twice the angle swept out between the turning points r_1 and r_2. Thus,

$$\Delta\phi = 2\ell \int_{r_1}^{r_2} \frac{dr}{r^2} \left[e^2 - \left(1 - \frac{2M}{r}\right)\left(1 + \frac{\ell^2}{r^2}\right)\right]^{-1/2}. \tag{9.51}$$

The turning points r_1 and r_2 are the places where $dr/d\tau$ vanishes along the orbit. From (9.26) these are places where the denominator of (9.51) vanishes. Thus, to find $\Delta\phi$ one has only to carry out the integral in (9.51) between the radii where the denominator vanishes. Figure 9.5 shows a plot of a numerical evaluation.

For applications in the solar system, $\Delta\phi$ needs to be evaluated only to the next order in $1/c^2$ after the Newtonian. To accomplish this, first put back in the factors of G and c^2 in (9.51), as described in the discussion leading to (9.32), to give

$$\Delta\phi = 2\ell \int_{r_1}^{r_2} \frac{dr}{r^2} \left[c^2\left(e^2 - 1\right) + \frac{2GM}{r} - \frac{\ell^2}{r^2} + \frac{2GM\ell^2}{c^2 r^3}\right]^{-1/2}. \tag{9.52}$$

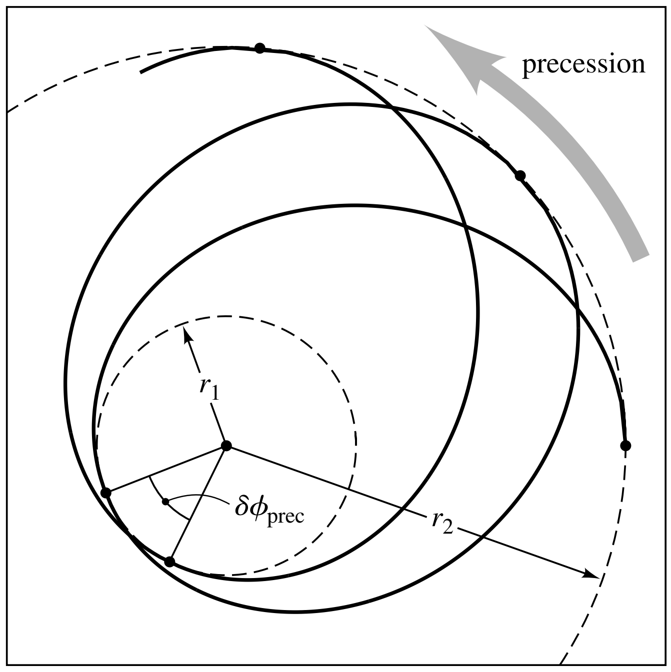

FIGURE 9.6 The shape of a bound orbit outside a spherical star. This is a picture of the orbital plane of the bound orbit whose radial motion is of the kind illustrated in the second pair of plots of Figure 9.4 The planet moves from a minimum radius r_1 out to a maximum radius r_2 and back to the same minimum radius. However, unlike the Keplerian ellipse of Newtonian gravitational theory, the orbit does not close. Rather, the angular position of the closest approach advances slightly on each return by an angle called the precession of the perihelion for a planet around the Sun. The figure shows a little over two orbits of a test mass that starts from the 3 o'clock position. The two positions of closest approach at the inner turning radius are indicated by dots. The angle between them is the precession of the perihelion per orbit.

In the bracket the constant term is not of order c^2, as it appears, but is of order unity, because from (9.31)

$$e^2 = 1 + \frac{2E_{\text{Newt}}}{mc^2} + \cdots \tag{9.53}$$

in an expansion in $1/c^2$. As we saw in (9.30), the first three terms in the bracket thus represent the Newtonian energy, gravitational potential, and centrifugal potential. The last term is of order $1/c^2$ with respect to the first three and represents the relativistic correction. It affects the orbits as a small additional $1/r^3$ term in the Newtonian potential would.

In the Newtonian approximation, in which the last term the denominator in (9.52) is negligible, it is not difficult to see that $\Delta\phi$ is exactly 2π and that, therefore, the orbits close. Neglecting the last term in the bracket, introducing a new variable $u = 1/r$ the integral in (9.52) can be rewritten in the form

$$\Delta\phi = 2\int_{u_2}^{u_1} \frac{du}{[(u_1 - u)(u - u_2)]^{1/2}}, \tag{9.54}$$

where $u_1 = 1/r_1$, $u_2 = 1/r_2$ ($u_1 > u_2$) are roots at which the quadratic expression in the denominator of (9.52) vanishes. This integral is easily looked up and the result is $\Delta\phi = 2\pi$ for all values of u_1 and u_2.

Expanding the integral (9.52) to find the first-order relativistic correction to the Newtonian result is a little tricky. You can read about one method of proceeding in Problem 15. By working through that problem you can find that after one orbit,

$$\delta\phi_{\text{prec}} = 6\pi\left(\frac{GM}{c\ell}\right)^2, \qquad \text{(first order in } 1/c^2\text{)}. \tag{9.55}$$

To this accuracy we can use the Newtonian orbits to evaluate ℓ in terms of the usual parameters: eccentricity, ϵ, and semimajor axis, a. Recall from your intermediate mechanics text that in Newtonian mechanics,

$$\ell^2 = \left(r^2\frac{d\phi}{d\tau}\right)^2 \approx \left(r^2\frac{d\phi}{dt}\right)^2 = GMa\left(1-\epsilon^2\right). \tag{9.56}$$

Thus,

Precession of the Perihelion

$$\boxed{\delta\phi_{\text{prec}} = \frac{6\pi G}{c^2}\frac{M}{a\left(1-\epsilon^2\right)}} \qquad \begin{pmatrix}\text{small } GM/c^2a \\ \text{per orbit}\end{pmatrix}. \tag{9.57}$$

This is the relativistic precession of the inner turning point of the Keplerian ellipse per orbit. When applied to the Sun, the inner turning point is called the perihelion, and this is the precession of a planet's perihelion.[3] The largest effect is for the smallest a—the planets closest to the Sun. For Mercury the predicted rate of precession is about 43 seconds of arc per century—a tiny number but one detected by precision measurements, as we see in the next chapter.

9.4 Light Ray Orbits—The Deflection and Time Delay of Light

The calculation of light ray orbits in the Schwarzschild geometry parallels the calculations of particle orbits, but with important differences. As discussed in Section 5.5 and Section 8.3, the world lines of light rays can be described by giving the coordinates x^α as functions of any one of a family of affine parameters λ. The null vector $u^\alpha \equiv dx^\alpha/d\lambda$ is tangent to the world line. Because the Schwarzschild metric is independent of t and ϕ, the quantities

$$e \equiv -\boldsymbol{\xi}\cdot\mathbf{u} = \left(1-\frac{2M}{r}\right)\frac{dt}{d\lambda}, \tag{9.58}$$

$$\ell \equiv \boldsymbol{\eta}\cdot\mathbf{u} = r^2\sin^2\theta\frac{d\phi}{d\lambda}, \tag{9.59}$$

[3] If it's a binary star system, the inner turning point is called the *periastron*.

are conserved along light ray orbits. These are the analogs of (9.21) and (9.22) in the particle case. Indeed, if the normalization of λ is chosen so that $\mathbf{u}$ coincides with the momentum $\mathbf{p}$ of a photon moving along the null geodesic, then e and ℓ are the photon's energy and angular momentum at infinity. A third integral is supplied by the requirement that the tangent vector be null [cf. (8.40)]:

$$\mathbf{u}\cdot\mathbf{u} = g_{\alpha\beta}\frac{dx^\alpha}{d\lambda}\frac{dx^\beta}{d\lambda} = 0. \tag{9.60}$$

The 0 rather than the -1 of (9.23) on the right-hand side of this equation is the only real difference between the particle case and the light ray case.

The derivation of an energy integral for the radial motion of light rays parallels the steps leading from (9.23) to (9.29). Writing out (9.60) for the orbit of a light ray in the equatorial plane $\theta = \pi/2$ gives

$$-\left(1-\frac{2M}{r}\right)\left(\frac{dt}{d\lambda}\right)^2 + \left(1-\frac{2M}{r}\right)^{-1}\left(\frac{dr}{d\lambda}\right)^2 + r^2\left(\frac{d\phi}{d\lambda}\right)^2 = 0. \tag{9.61}$$

Using (9.58) and (9.59) to eliminate $dt/d\lambda$ and $d\phi/d\lambda$, respectively, we have

$$-\left(1-\frac{2M}{r}\right)^{-1}e^2 + \left(1-\frac{2M}{r}\right)^{-1}\left(\frac{dr}{d\lambda}\right)^2 + \frac{\ell^2}{r^2} = 0. \tag{9.62}$$

Multiplying by $(1-2M/r)/\ell^2$, this can be put in the form

$$\boxed{\frac{1}{b^2} = \frac{1}{\ell^2}\left(\frac{dr}{d\lambda}\right)^2 + W_{\text{eff}}(r).} \tag{9.63}$$

Here

$$b^2 \equiv \ell^2/e^2, \tag{9.64}$$

and

$$\boxed{W_{\text{eff}}(r) \equiv \frac{1}{r^2}\left(1-\frac{2M}{r}\right).} \tag{9.65}$$

Effective Potential for Photon Orbits

Equation (9.63) has the form of an energy integral for radial motion with $W_{\text{eff}}(r)$ playing the role of the effective potential and b^{-2} playing the role of the energy. This relation can be used to analyze light ray orbits in much the same way that (9.29) was used to analyze particle orbits. However, unlike the particle case, where distinct values of e and ℓ determined different orbits, the physical properties of light ray orbits can depend only on their ratio, ℓ/e. That is because of the freedom in normalizing the affine parameter, λ. If λ is multiplied by a constant

K, it is just as good an affine parameter because (9.60) and the geodesic equation (8.42) are still satisfied. Physical predictions can't change by changing the affine parameter in this way, but e and ℓ are each divided by K. Therefore, only the ratio ℓ/e has physical significance and determines the properties of light ray orbits. Calculations of physical properties of light ray orbits, such as their shape, should automatically yield a result that depends only on the ratio ℓ/e. If they don't, there is a mistake in the calculation!

The sign of ℓ indicates which way the light ray is going around the center of attraction. We'll define $b \equiv |\ell/e|$ since that is what the shape of the orbits depend on. To see what b is, consider orbits that reach infinity. At infinity space is flat and Cartesian coordinates can be introduced that are related to Schwarzschild polar coordinates in the usual way, e.g., in the equatorial plane

$$x = r\cos\phi, \qquad y = r\sin\phi. \tag{9.66}$$

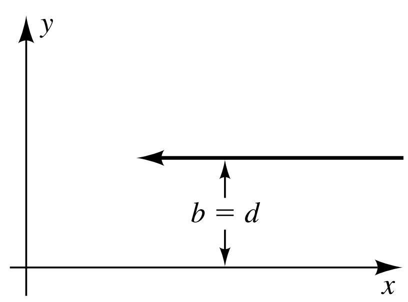

FIGURE 9.7 A segment of the orbit of an inwardly directed light ray far from the source of gravitational attraction is shown in this plot using Cartesian coordinates defined in (9.66). The light ray is moving inward on a straight line with speed 1 a distance d from the x-axis through the center of spherical symmetry. This distance is the *impact parameter* and is $b \equiv |\ell/e|$, as demonstrated in the text.

Consider a light ray moving parallel to the x-axis a distance of d away from it, as shown in Figure 9.7. Far away from the source of curvature, the light ray is moving in a straight line. For $r \gg 2M$, the quantity b is

$$b \equiv \left|\frac{\ell}{e}\right| \approx \frac{r^2 d\phi/d\lambda}{dt/d\lambda} = r^2\frac{d\phi}{dt}. \tag{9.67}$$

For very large r we have $\phi \approx d/r$, and $dr/dt \approx -1$, giving

$$\frac{d\phi}{dt} = \frac{d\phi}{dr}\frac{dr}{dt} = \frac{d}{r^2}. \tag{9.68}$$

Thus,

$$b = d. \tag{9.69}$$

The constant b is thus the *impact parameter* of a light ray that reaches infinity. It is defined to be positive. In geometrized units b has dimensions of length from (9.67). We will define it so it has the dimensions of length in any system of units as is appropriate for an impact parameter. Thus in $c \neq 1$ units $b \equiv |\ell/(ce)|$.

The plots on the left-hand side of Figure 9.8 show the shape of $W_{\text{eff}}(r)$. It vanishes at large r and has one maximum at $r = 3M$. The height at the maximum is

$$W_{\text{eff}}(3M) = \frac{1}{27M^2}. \quad \text{(maximum of } W_{\text{eff}}\text{)} \tag{9.70}$$

Circular orbits of light rays of radius $r = 3M$ are possible at this maximum if $b^2 = 27M^2$. However, these circular orbits are unstable since a small change in b results in an orbit that moves away from the maximum. A circular light ray orbit would not be possible around the Sun because the solar radius is much larger than $3M_\odot \approx 4.5$ km, but, as we'll see in Chapter 12, there can be circular light ray orbits outside a black hole.

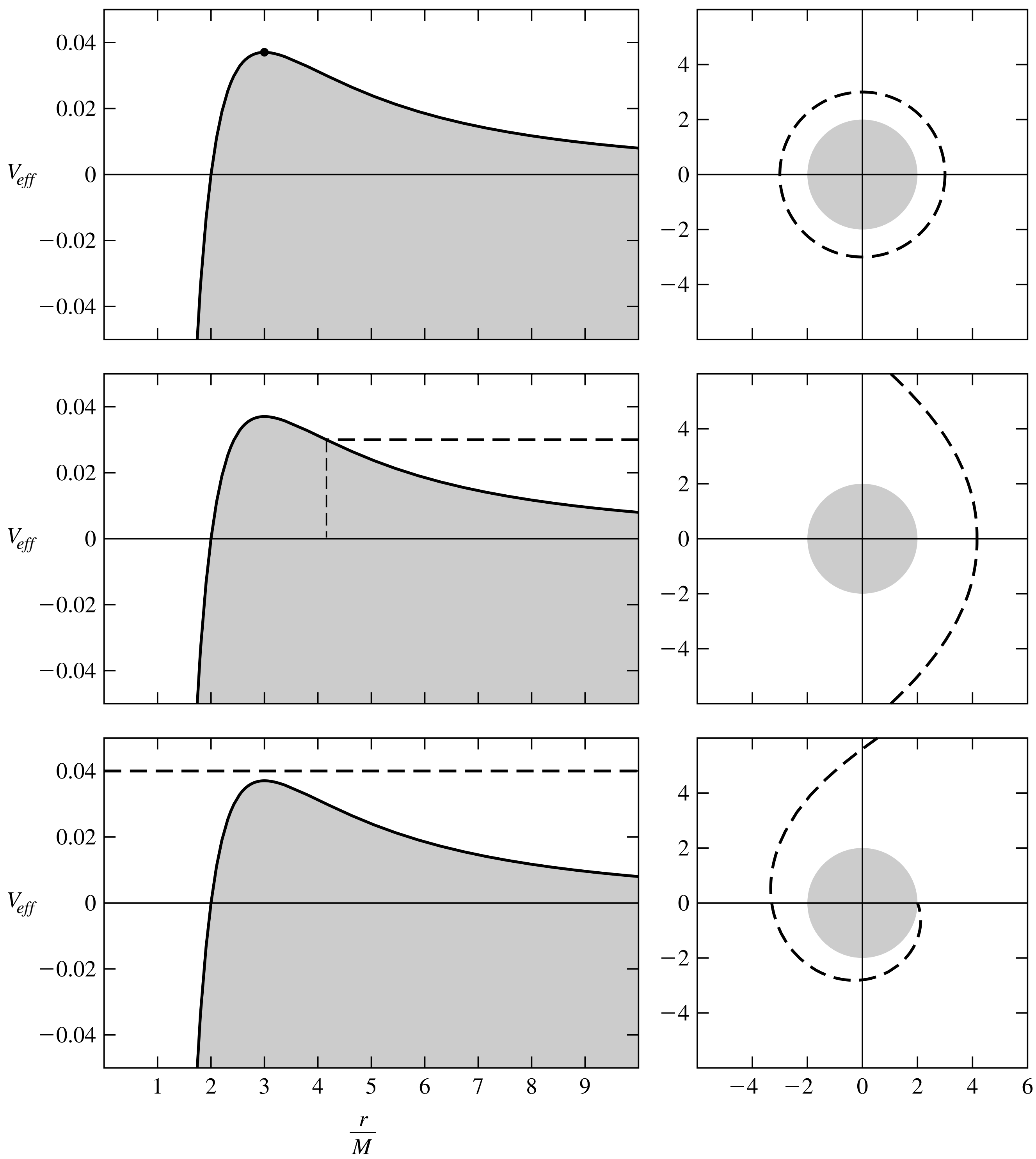

FIGURE 9.8 Three kinds of light ray orbits in the Schwarzschild geometry. The figure shows three orbits corresponding to different values of b. The potential and its relationship to $1/b^2$ are shown at left. The horizontal axis is r/M. The vertical axis is $W_{\text{eff}}(r)$. The heavy doted lines are the values of $1/b^2$. The shape of the orbit at right. From the top down there are a circular orbit, a scattering orbit, and a plunge orbit.

The qualitative character of other light ray orbits depends on whether $1/b^2$ is greater or less than the maximum height of W_{eff}, as shown in Figure 9.8. First consider orbits that start from infinity. If $1/b^2 < 1/(27M^2)$, then the orbit will have a turning point and again escape to infinity, as in the second of the examples in Figure 9.8. The light from a star being bent around the Sun is following one

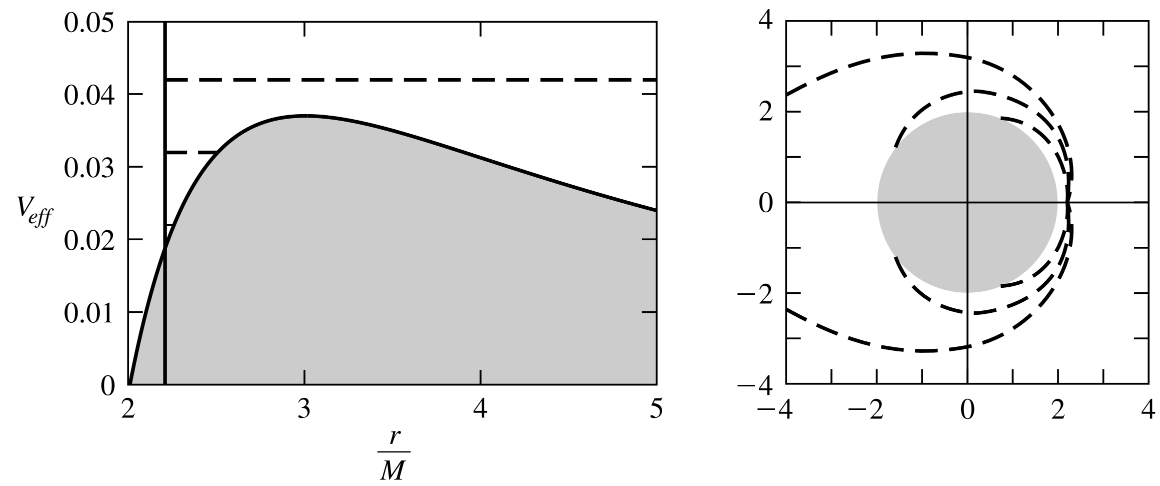

FIGURE 9.9 Light rays emitted between $r = 2M$ and $r = 3M$. A stationary observer at a radius $r = R = 2.2M$ emits light rays in various different outward directions corresponding to different values of b^2. This figure shows what happens to three cases $(M/b)^2 = .022, .032, .042$—values that were chosen to make intelligible plots. The left-hand plot shows a detail of the effective potential $W_{\text{eff}}(r)$ together with a vertical line marking $r = 2.2M$ and horizontal lines marking the various values of b^{-2}. The right-hand plot shows the equatorial plane spanned by the Cartesian (x, y) defined in (9.66), together with the orbits of pairs of light rays with these values of b^{-2} emitted in directions above and below the x-axis. A radial light ray with $b \equiv |\ell/e| = 0$ or infinite b^{-2} (not shown) will escape. Light rays with values of b^{-2} higher than the maximum of the barrier $1/(27M^2) = .037/M^2$, making sufficiently small angles with the radial direction, will also escape like the pair with the value $(M/b)^2 = .042$ illustrated. Light rays with values of b^{-2} less than the height of the barrier will not escape. They move outward for a bit but then fall back through the radius $r = 2M$ like the pairs with the values $(M/b)^2 = .022, .032$. There is thus a critical angle ψ_{crit} with respect to the radial direction such that light rays emitted with less than this angle escape, but those with greater than this angle to not. Its value is given in (9.74). As $R \to 2M$, the opening angle for escaping light rays goes to zero, and essentially no light can escape.

of these scattering orbits, and measurements of the amount of deflection is an important test of general relativity, as we will see shortly. If $1/b^2 > 1/(27M^2)$, then the light ray will plunge all the way into the origin and be captured, as in the last pair in Figure 9.8.

Similar considerations hold for trajectories that start at small radii between $r = 2M$ and $r = 3M$, as shown in Figure 9.9. If $1/b^2 > 1/(27M^2)$, the light ray will escape. If $1/b^2 < 1/(27M^2)$ there is a turning point and the light ray falls back onto the center of attraction. Since $b^2 = \ell^2/e^2$, these criteria mean that if the light ray starts with sufficiently small angular momentum, i.e., is aimed sufficiently near the radial direction, then it will escape. Otherwise it falls back on the source of attraction. The situation is illustrated in Figure 9.9 and discussed quantitatively in Example 9.2.

Example 9.2. How Much Light Escapes to Infinity? A stationary observer stationed at a radius $R < 3M$ sends out light rays in various directions in the equatorial plane $\theta = \pi/2$, making angles ψ with the radial direction. Radial light rays with $\psi = 0$ have $b = 0$ and escape. What is the critical angle ψ_{crit} beyond which the light rays will fall back into the center of attraction, as illustrated in Figure 9.9? The answer depends on the connection between b and ψ, which can be found by analyzing the initial velocity of the light ray in an orthonormal basis $\{\mathbf{e}_{\hat{\alpha}}\}$ associated with the laboratory of the observer. The vector $\mathbf{e}_{\hat{0}}$ is the observer's timelike four-velocity and points along the t-direction. It is simplest to choose the three spacelike basis vectors to be oriented along the orthogonal coordinate axes at the position of the observer. Denote these by $\mathbf{e}_{\hat{r}}$, $\mathbf{e}_{\hat{\theta}}$, and $\mathbf{e}_{\hat{\phi}}$. In this orthonormal basis the angle between the direction of the light ray and the radial direction is given by

$$\tan\psi = \frac{u^{\hat{\phi}}}{u^{\hat{r}}} = \frac{\mathbf{u}\cdot\mathbf{e}_{\hat{\phi}}}{\mathbf{u}\cdot\mathbf{e}_{\hat{r}}}, \tag{9.71}$$

where the connection between orthonormal basis components and inner products with basis vectors in (5.82) has been used. To calculate the scalar products in (9.71) the coordinate basis components of the basis vectors $\mathbf{e}_{\hat{r}}$ and $\mathbf{e}_{\hat{\phi}}$ are needed in the equatorial plane along with the coordinate basis components of $\mathbf{u}$ given by (9.22) and (9.29). These components of the basis vectors can be found by following Example 7.9, and are

$$(\mathbf{e}_{\hat{r}})^{\alpha} = [0, (1 - 2M/R)^{1/2}, 0, 0], \tag{9.72a}$$

$$(\mathbf{e}_{\hat{\phi}})^{\alpha} = [0, 0, 0, 1/R], \tag{9.72b}$$

where the components are listed in the order (t, r, θ, ϕ). The scalar products in (9.71) can then be computed utilizing (7.57), (9.10), (9.60), (9.63), and (9.72), with the following results:

$$\mathbf{u}\cdot\mathbf{e}_{\hat{\phi}} = g_{\phi\phi}(\mathbf{e}_{\hat{\phi}})^{\phi}u^{\phi} = \frac{\ell}{R}, \tag{9.73a}$$

$$\mathbf{u}\cdot\mathbf{e}_{\hat{r}} = g_{rr}(\mathbf{e}_{\hat{r}})^{r}u^{r} = \left(1 - \frac{2M}{R}\right)^{-1/2}\ell\left[\frac{1}{b^2} - \frac{1}{R^2}\left(1 - \frac{2M}{R}\right)\right]^{1/2}. \tag{9.73b}$$

The ratio of these gives $\tan\psi$, according to (9.71). The critical opening angle ψ_{crit} below which light rays escape to infinity occurs when $b^2 = 27M^2$:

$$\tan\psi_{\text{crit}} = \frac{1}{R}\left(1 - \frac{2M}{R}\right)^{1/2}\left[\frac{1}{27M^2} - \frac{1}{R^2}\left(1 - \frac{2M}{R}\right)\right]^{-1/2}. \tag{9.74}$$

(Recall that $2M < R < 3M$.)

At $R = 3M$ the quantity in the square bracket vanishes because that's the maximum of the effective potential $1/(27M^2)$. There $\psi_{\text{crit}} = \pi/2$. That is just what could be expected from the existence of the circular orbit at that radius. The light ray making the circular orbit is just on the borderline between escaping to infinity and falling into the center of attraction. As R decreases below $3M$, the critical angle gets less and less until finally it vanishes altogether at $R = 2M$. At that point, no light gets out except the exactly radial light ray. Viewed from the exterior, a flashlight held by the stationary observer at radius R and emitting in all directions would appear dimmer and dimmer as R approaches $2M$. This anticipates the black hole phenomenon discussed in Chapter 12.

The Deflection of Light

From the discussion of light rays proceeding from infinity with a large impact parameter, it is evident that all material bodies will bend light trajectories somewhat. This effect is important because the deflection of light by the Sun is one of the most important experimental tests of general relativity, and the deflection of light by galaxies is the mechanism behind gravitational lenses to be discussed in the next chapter. The angle of interest is the deflection angle $\delta\phi_{\text{def}}$, defined as in Figure 9.10. This angle is a property of the shape of the orbit of a light ray. The shape of a light ray orbit can be calculated in the same way as the shape of a particle orbit. Solve (9.59) for $d\phi/d\lambda$, solve (9.63) for $dr/d\lambda$, divide the second into the first, and then simplify using (9.64) and (9.65) to find

$$\frac{d\phi}{dr} = \pm\frac{1}{r^2}\left[\frac{1}{b^2} - W_{\text{eff}}(r)\right]^{-1/2}. \tag{9.75}$$

The sign gives the direction of the orbit; integration gives its shape. In particular, the magnitude of the total angle swept out as the light ray proceeds in from infinity and back out again $\Delta\phi$ is just twice the angle swept out from the turning point $r = r_1$ to infinity. Thus,

$$\Delta\phi = 2\int_{r_1}^{\infty}\frac{dr}{r^2}\left[\frac{1}{b^2} - \frac{1}{r^2}\left(1 - \frac{2M}{r}\right)\right]^{-1/2}. \tag{9.76}$$

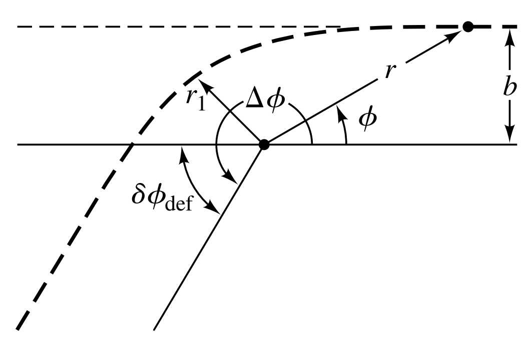

FIGURE 9.10 Quantities needed for calculating the deflection of light $\delta\phi_{\text{def}}$ by a spherical star. In this schematic diagram a light ray enters at right with an impact parameter b corresponding to a scattering orbit as in the second pass of plots in Figure 9.8. It approaches the center of attraction until the turning point at $r = r_1$, after which it moves out to infinity, emerging deflected by an angle $\delta\phi_{\text{def}}$. That deflection angle is the total angle swept out in the orbit $\Delta\phi$ less π.

The turning point r_1 is the radius where $1/b^2 = W_{\text{eff}}(r_1)$, i.e., the radius where the bracket in the preceding expression vanishes. By introducing a new variable w defined by

$$r = (b/w), \tag{9.77}$$

the expression for $\Delta\phi$ becomes

$$\Delta\phi = 2\int_0^{w_1} dw \left[1 - w^2\left(1 - \frac{2M}{b}w\right)\right]^{-1/2} \tag{9.78}$$

where w_1 is the value of w at which the bracket vanishes. The angle $\Delta\phi$ swept out in one pass thus depends only on the ratio M/b. A plot of its behavior for large values of this ratio is shown in Figure 9.11.

For the bending of light by the Sun, the smallest value for b is approximately the solar radius $R_\odot = 6.96\times10^5$ km, whereas $M_\odot = 1.47$ km. The value of $2M/b$ is $\sim 10^{-6}$. The integral (9.78) can be expanded in powers of $2M/b$ to find an analytic expression for the deflection adequate for such small values. Expanding the integral requires a trick similar to the one needed for the expansion of (9.52), but since the algebra is not as messy we include a few steps to show how it goes. First rewrite (9.78) in the form

$$\Delta\phi = 2\int_0^{w_1} dw \left(1 - \frac{2M}{b}w\right)^{-1/2}\left[\left(1 - \frac{2M}{b}w\right)^{-1} - w^2\right]^{-1/2}. \tag{9.79}$$

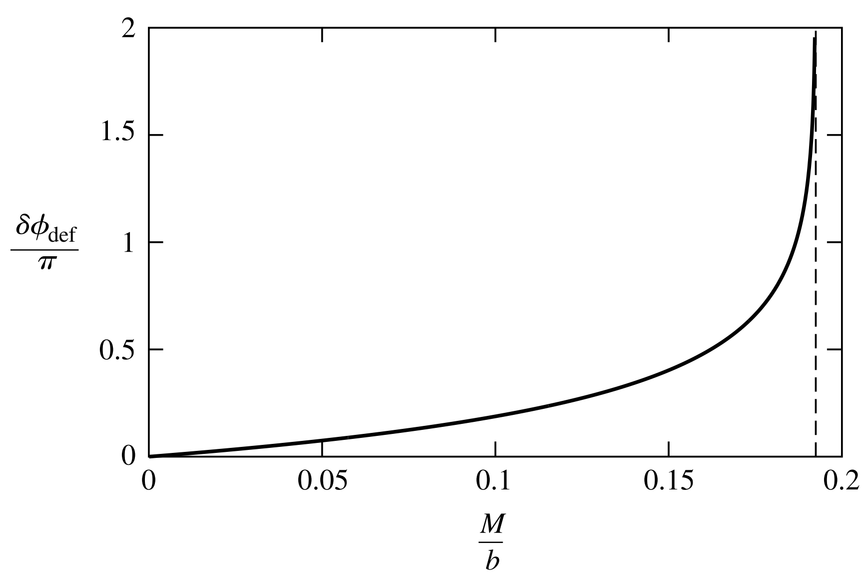

FIGURE 9.11 The deflection of light as a function of impact parameter. This is a rough plot of the angle $\delta\phi_{\text{def}}$ defined by (9.82) and the integral in (9.78) as a function of M/b. For values of $M/b < 2\times10^{-6}$ that are relevant for the deflection of light by the Sun, the linear approximation (9.83) is more than adequate. The deflection angle increases with smaller b, becoming infinite at the value $\sqrt{27}M$ at which an incoming photon would be injected into a circular orbit.

Next expand both inverse factors of $1 - (2M/b)w$ in powers of $2M/b$ and keep only the linear terms. The result is

$$\Delta\phi = 2\int_0^{w_1} dw \frac{1 + (M/b)w}{\left[1 + (2M/b)w - w^2\right]^{1/2}}, \tag{9.80}$$

w_1 being all along a root of the denominator. The integral is now in a form where it can be looked up in a table or done using an algebraic integration program. The result is

$$\Delta\phi \approx \pi + \frac{4M}{b} \tag{9.81}$$

for small M/b. From Figure 9.10 we see that the deflection angle $\delta\phi_{\text{def}}$ is related to $\Delta\phi$ by

$$\delta\phi_{\text{def}} = \Delta\phi - \pi. \tag{9.82}$$

Thus,

$$\delta\phi_{\text{def}} = \frac{4M}{b} \quad \text{(small } M/b\text{)}. \tag{9.83}$$

This is the relativistic deflection of light when M/b is small. Reinserting the factors of G and c, it can also be written (remember b has dimensions of length)

Deflection of light

$$\boxed{\delta\phi_{\text{def}} = \frac{4GM}{c^2 b}} \quad \text{(small } GM/c^2 b\text{)}. \tag{9.84}$$

For a light ray just grazing the edge of the Sun, the deflection angle is $1.7''$ ($''$ is the standard notation for seconds of arc). We discuss how that's measured in the next chapter.

The Time Delay of Light

Another interesting relativistic effect found in the propagation of light rays is the apparent delay in propagation time for a light signal passing near the Sun. This is important because radar-ranging techniques can measure this delay and give another test of general relativity, and the time delay of light is a relevant correction for other observations. The effect is called the *Shapiro time delay* after Irwin Shapiro (1929–) who predicted it and led the first measurements of it to test general relativity. To see what's involved, imagine the following experiment: a radar signal is sent from the Earth to pass close to the Sun and reflect off another planet or a spacecraft. The time interval between the emission of the first pulse and the reception of the reflected pulse is measured. What does relativity predict for this number? We already have the machinery to answer this question.

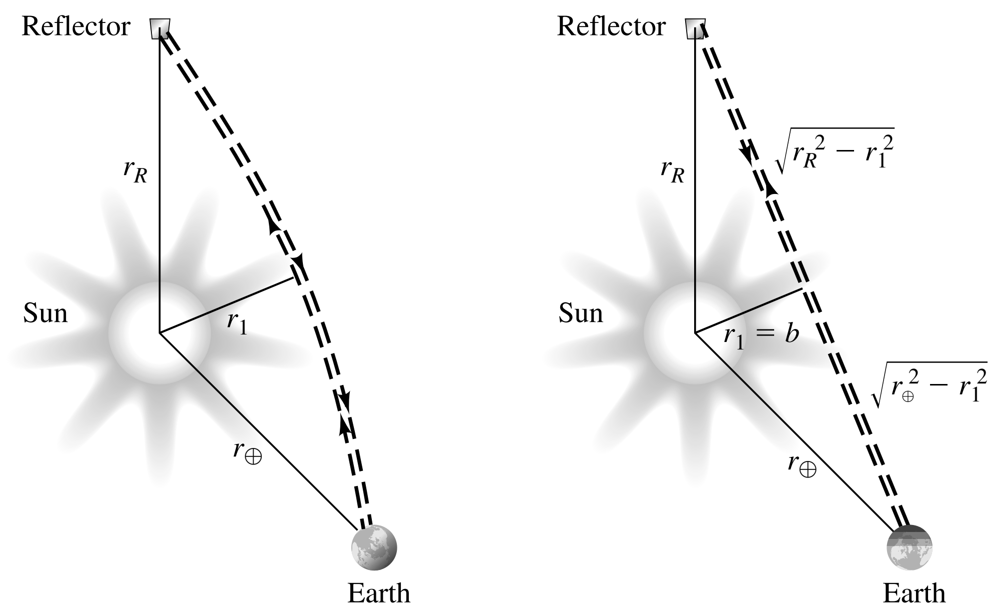

FIGURE 9.12 At left is a schematic diagram of the radar-ranging time delay experiment. Radar waves are sent from the Earth to a distant reflector so that they pass close to the Sun. They are deflected as all electromagnetic radiation is. There is an excess time delay between sending and return above what would be expected were the signals propagating along straight lines in flat spacetime as shown in the right-hand figure. That time delay caused by the curvature of the spacetime in the vicinity of the Sun is an important test of general relativity.

The geometry of the situation is illustrated in Figure 9.12. The path of the radar signals will be curved because they are deflected by the Sun, although we have greatly exaggerated the effect in the figure. The quantities $r_\oplus$ and r_R are radii of the Earth and the reflector, respectively, in Schwarzschild coordinates centered on the Sun. These are not enough to specify the orbit because they do not fix the orientation of the planets relative to the Sun. Only one other distance is needed to do this, and we choose it to be the Schwarzschild radius of closest approach, r_1.

The Earth can be thought of as stationary over the round-trip travel time of the pulse (about 41 min). The total time interval between the emission and return of a pulse as measured by a clock on Earth is the Schwarzschild coordinate time interval $(\Delta t)_{\text{total}}$ between these events corrected for the influence of the Earth on spacetime and other effects. To calculate $(\Delta t)_{\text{total}}$ we need t as a function of r along the path of the pulse. This is like finding the shape of the orbit in the t-r plane and can be found in much the same way that we found ϕ as a function of r for the deflection problem. Solve (9.58) for $dt/d\lambda$ and (9.63) for $dr/d\lambda$ and divide the second into the first to find

$$\frac{dt}{dr} = \pm\frac{1}{b}\left(1 - \frac{2M}{r}\right)^{-1}\left[\frac{1}{b^2} - W_{\text{eff}}(r)\right]^{-1/2}, \tag{9.85}$$

where the $+$ sign is appropriate for when the radius is increasing and the $-$ sign applies when it is decreasing. Over the whole of the pulse's trajectory, the radius decreases from $r_\oplus$ to a minimum value r_1 at the turning point—the point of closest approach—and then increases again to r_R. On the return journey the pulse repeats this sequence in inverse order. The total elapsed time is

$$(\Delta t)_{\text{total}} = 2t\,(r_{\oplus}, r_1) + 2t\,(r_R, r_1)\,, \tag{9.86}$$

where $t(r, r_1)$ is the travel time from the turning point r_1 to a radius r given by

$$t(r, r_1) = \int_{r_1}^{r} dr \frac{1}{b}\left(1 - \frac{2M}{r}\right)^{-1}\left[\frac{1}{b^2} - W_{\text{eff}}(r)\right]^{-1/2}. \tag{9.87}$$

The parameters b and r_1 are related by

$$\frac{1}{b^2} = W_{\text{eff}}\,(r_1)\,. \tag{9.88}$$

For solar system experiments we need to evaluate the integral in (9.87) only to first order in M. The integral can be carried out in that approximation by expanding the integrand similarly to the case of the defection of light (9.79). Equation (9.88) shows that to first order in M,

$$b = r_1 + M + \cdots\,, \tag{9.89}$$

where the neglected terms are of order $M(M/r_1)$. This result can be used to eliminate b from the answer. The result is

$$t(r, r_1) = \sqrt{r^2 - r_1^2} + 2M \log\left[\frac{r + \sqrt{r^2 - r_1^2}}{r_1}\right] + M\left(\frac{r - r_1}{r + r_1}\right)^{1/2}. \tag{9.90}$$

The first term in this expression is the Newtonian expression for the propagation time, as is seen from right-hand figure in Figure 9.12. The next terms represent the relativistic corrections, which increase the propagation time over the Newtonian value. The total time delay is obtained by substituting (9.90) in (9.86).

This division of the time delay into a Newtonian contribution and relativistic correction depends crucially the use of the Schwarzschild radial coordinate in (9.90). Make a small change in the radial coordinate by an amount proportional to M and this division would change. Only the total elapsed time that is measured is a physical quantity. Nevertheless, the experimental results are usually quoted in terms of the *excess delay* over that which would be expected in Newtonian theory (see Figure 9.12) using Schwarzschild coordinates and (9.90):

$$(\Delta t)_{\text{excess}} \equiv (\Delta t)_{\text{total}} - 2\sqrt{r_{\oplus}^2 - r_1^2} - 2\sqrt{r_R^2 - r_1^2}. \tag{9.91}$$

The biggest effect occurs when r_1 is close to the solar radius. For $r_1/r_R \ll 1$ and $r_1/r_{\oplus} \ll 1$, expression (9.91) simplifies to give to a good approximation:

Time Delay of Light

$$\boxed{(\Delta t)_{\text{excess}} \approx \frac{4GM}{c^3}\left[\log\left(\frac{4r_R r_{\oplus}}{r_1^2}\right) + 1\right],} \tag{9.92}$$

where the factors of G and c have been reinserted. We describe the comparison of this expression with experiment in the next chapter.

Results like these for the time intervals measured by particular observers for light to travel over large distances do not mean that the velocity of light differs from c in general relativity. If you take 10 days to cross the United States it does not mean that your velocity is the distance traveled divided by 10 days. Velocity is a property of *each point* of a trajectory in Newtonian mechanics, special relativity, and general relativity. As discussed in Section 7.5, the local light cone structure of spacetime guarantees that velocity is always c for light as summarized by the condition that the four-velocity of a light ray is null: $\mathbf{u} \cdot \mathbf{u} = 0$ at each point along its world line.

Problems

1. [S] An advanced civilization living outside a spherical neutron star of mass M constructs a massless shell concentric with the star such that the area of the inner surface is $144\pi M^2$ and the area of the outer surface is $400\pi M^2$. What is the physical thickness of the shell?

2. Positrons are produced in the dense plasma surrounding a neutron star, which is accreting material from a binary companion, and electrons and positrons annihilate to produce γ rays. Assuming the neutron star has a mass of $2.5M_\odot$ (solar masses) and a radius of 10 km, at what energy should a distant observer look for the γ rays being emitted from the star by this process? Assume the center of mass of the electron and positron is at rest with respect to the star when they annihilate.

3. An observer is stationed at fixed radius R in the Schwarzschild geometry produced by a spherical star of mass M. A proton moving radially outward from the star traverses the observer's laboratory. Its energy E and momentum $|\vec{P}|$ are measured.

(a) What is the connection between E and $|\vec{P}|$?

(b) What are the components of the four-momentum of the proton in the Schwarzschild coordinate basis in terms of E and $|\vec{P}|$?

4. [B, E] Suppose the shell discussed in Box 9.1 on p. 192 is to be designed so the g-forces experienced by an observer falling into the shell are to be less than $20g$, where $g = 9.8$ m/s^2. If the observer falls feet first into the shell, these g-forces are the *difference* between the force per unit mass at the observer's head and feet. *Estimate* using Newtonian theory how massive and how big would the shell have to be to meet this design criterion.

5. Sketch the qualitative behavior of a particle orbit that comes in from infinity with a value of $\mathcal{E}$ exactly equal to the maximum of the effective potential, V_{eff}. How does the picture change if the value of $\mathcal{E}$ is a little bit larger than the maximum or a little bit smaller?

6. [S] An observer falls radially inward toward a black hole of mass M (exterior geometry the Schwarzschild geometry), starting with zero kinetic energy at infinity. How much time does it take, as measured on the observer's clock, to pass between the radii $6M$ and $2M$?

7. Two particles fall radially in from infinity in the Schwarzschild geometry. One starts with $e = 1$, the other with $e = 2$. A stationary observer at $r = 6M$ measures the speed of each when they pass by. How much faster is the second particle moving at that point?

8. A spaceship is moving without power in a circular orbit about a black hole of mass M. (The exterior geometry is the Schwarzschild geometry.) The Schwarzschild radius of the orbit is $7M$.

(a) What is the period of the orbit as measured by an observer at infinity?

(b) What is the period of the orbit as measured by a clock in the spaceship?

9. Find the relation between the rate of change of angular position of a particle in a circular orbit with respect to proper time and the Schwarzschild radius of the orbit. Compare with (9.46).

10. Find the linear velocity of a particle in a circular orbit of radius R in the Schwarzschild geometry that would be measured by a stationary observer stationed at one point on the orbit. What is its value at the ISCO?

11. A small perturbation of an unstable circular orbit will grow exponentially in time. Show that a displacement δr from the unstable maximum of the Schwarzschild will grow initially as

$$\delta r \propto e^{\tau/\tau_*},$$

where τ is the proper time along the particle's trajectory and τ_* is a constant. Evaluate τ_*. Explain its behavior as the radius of the orbit approaches $6M$.

12. A comet starts at infinity, goes around a relativistic star and goes out to infinity. The impact parameter at infinity is b. The Schwarzschild radius of closest approach is R. What is the speed of the comet at closest approach as measured by a stationary observer at that point?

13. [N, C] Particle orbits in the Schwarzschild geometry generally do not close after one turn. Explain why there should be a set of values $\mathcal{E}(\ell)$ for which orbits close for a given number of turns greater than one. Using the *Mathematica* program on the book website or otherwise find a value of $\mathcal{E}$ for which the orbit closes after four turns when $\ell = 4.6$ making a kind of clover leaf pattern.

14. In Newtonian mechanics one of Kepler's laws says that equal areas are swept out in equal time as a particle moves around an elliptical orbit in a $1/r$ potential. Consider the area outside a radius $R > 2M$ that is swept out by an orbit in the Schwarzschild geometry that stays outside this radius. Does Kepler's area law hold true using either proper time or Schwarzschild time?

15. [A] *Precession of the Perihelion of a Planet* To find the first order in $1/c^2$ relativistic correction to the angle $\Delta\phi$ swept out by in one bound orbit, one might be be tempted to expand the integrand in (9.52) in the small quantity $2GM\ell^2/c^2r^3$ and keep only the first two terms. This would be a mistake because the resulting integral would diverge near a turning point such as $\int^{r_2} dr/(r_2 - r)^{3/2}$, whereas the original integral is finite. There are several ways of rewriting the integrand so it can be expanded. One trick is to factor $(1 - 2GM/c^2r)$ out of the denominator so that it can be written

$$\Delta\phi = 2\ell \int_{r_1}^{r_2} \frac{dr}{r^2}\left(1 - \frac{2GM}{c^2r}\right)^{-1/2}\left[c^2e^2\left(1 - \frac{2GM}{c^2r}\right)^{-1} - \left(c^2 + \frac{\ell^2}{r^2}\right)\right]^{-1/2}.$$

The factor in the brackets is then still the square root of a quantity quadratic in $1/r$ to order $1/c^2$. To derive the expression (9.55) evaluate this expression as follows.

(a) Expand the factors of $(1-2GM/c^2r)$ in the preceding equation in powers of $1/c^2$, keeping only the $1/c^2$ corrections to Newtonian quantities and using (9.53).

(b) Introduce the integration variable $u = 1/r$, and show that the integral can be put in the form

$$\Delta\phi = \left[1 + 2\left(\frac{GM}{c\ell}\right)^2\right] 2\int_{u_2}^{u_1} \frac{du}{\left[(u_1 - u)(u - u_2)\right]^{1/2}} + \frac{2GM}{c^2}\int_{u_2}^{u_1} \frac{u\,du}{\left[(u_1 - u)(u - u_2)\right]^{1/2}} + \begin{pmatrix}\text{higher} \\ \text{order in } 1/c^2\end{pmatrix}.$$

(c) The first integral (including the 2) is just the one in (9.54) and equals 2π. Show that the second integral gives $(\pi/2)(u_1 + u_2)$ and that this equals $\pi\, GM/\ell^2$ to lowest order in $1/c^2$.

(d) Combine these results to derive (9.55).

16. A beam of photons with a circular cross section of radius a is aimed toward a black hole of mass M from far away. The center of the beam is aimed at the center of the black hole. What is the largest radius $a = a_{\max}$ of the beam such that all the photons in the beam are captured by the black hole? The capture cross section is $\pi a_{\max}^2$.

17. Calculate the deflection of light in Newtonian gravitational theory assuming that the photon is a "nonrelativistic" particle that moves with speed c when far from all sources of gravitational attraction. Compare your answer to the general relativistic result.

18. Suppose in another theory of gravity (not Einstein's general relativity) the metric outside a spherical star is given by

$$ds^2 = \left(1 - \frac{2M}{r}\right)\left[-dt^2 + dr^2 + r^2(d\theta^2 + \sin^2\theta\, d\phi^2)\right].$$

Calculate the deflection of light by a spherical star in this theory assuming that photons move along null geodesics in this geometry and following the steps that led to (9.78). When you get the answer see if you can find a simpler way to do the problem.

19. [N] Write a *Mathematica* program for the *null* geodesics in the Schwarzschild geometry analogous to the one on the website for particle geodesics. Use this program to illustrate the orbits with impact parameters a little above and a little below the critical impact parameter for a circular orbit.

20. **(a)** What is the speed of a particle in the smallest possible unstable circular orbit in the Schwarzschild geometry as measured by a stationary observer at that radius?

(b) What is the connection of this orbit to the unstable circular orbit of a photon in the Schwarzschild geometry?

21. [E] Suppose a neutron star were luminous so that features on its surface could be viewed with a telescope. The gravitational bending of light means that not only the hemisphere pointing toward us could be seen but also part of the far hemisphere.

Explain why and *estimate* the angle measured from the line the extension of sight on the far side above which the surface could be seen. This would be $\pi/2$ if there were no bending, but less than that because of the bending. A typical neutron star has a mass of $\sim M_{\odot}$ and a radius of ~ 10 km.

22. [N, C] *Looking for Black Holes with Lasers* Suppose primordial black holes of mass $\sim 10^{15}$ g were made in the early universe and are now distributed throughout space. If an observer shines a laser on a black hole some of the light is backscattered to the observer. A search for such primordial black holes could in principle be carried out by shining lasers into space and looking for the backscattered radiation.

(a) Explain why some light is backscattered.

(b) Suppose the flux of photons $[(\text{number})/\text{m}^2 \cdot \text{s}]$ in the laser beam is f_*, the mass of the black hole is M, and it is a distance R away. Derive a formula for the number of photons per second that will be returned to a collecting area of radius d at the origin of the beam. Assume that the width of the beam is much larger than the size of the black hole. (*Hint*: A little numerical integration is required to get an accurate answer for this problem.)

(c) Could the lasers described in Box 2.1 on p. 14 hope to detect such a black hole?